COBEM 2021 26th International Congress of Mechanical Engineering
November 22-26, 2021, Virtual Congress, Brazil

COB-2021-1556
FLOW BOILING OF R1336mzz(Z) IN OPEN MICROCHANNELS WITH DIVERGING MANIFOLD

Debora C. Moreira
Valter S. do Nascimento Jr.
Gherhardt Ribatski
Heat Transfer Research Group, Department of Mechanical Engineering, São Carlos School of Engineering, University of São Paulo
dcmoreira@usp.br, nascimento.valter@usp.br, ribatski@sc.usp.br

Satish G. Kandlikar
Thermal Analysis, Microfluidics, and Fuel Cells Laboratory, Mechanical Engineering Department, Rochester Institute of Technology
sgkeme@rit.edu

Abstract. *The advances in electronics and miniaturization of components is directly related to an increasing demand for high heat flux dissipation technologies. Among many existing techniques used to dissipate high heat fluxes, heat sinks based on flow boiling in microchannels is one of the most promising ones, given the possibility of reaching extremely high values of critical heat flux (CHF) that have already surpassed 1 kW/cm^2, with huge values of heat transfer coefficient (HTC) and minimum temperature variation along the devices. In this context, over the last decades many efforts have been made to develop these heat sinks, revealing mechanisms that can be altered to enhance flow boiling heat transfer. The use of open and diverging manifold over microchannels as a vapor venting technique resulted in simultaneous augmentation of HTC and CHF with reduction in pressure drop, and can be applied over any array of channels or pillars, but there is limited data on experiments with refrigerant fluids in such configuration. In this work the flow boiling behavior of the refrigerant R1336mzz(Z) in a microchannels-based heat sink with an open and divergent manifold was investigated. The test section comprises a copper chip with milled microchannels and a polysulfone cover with a diverging open section above the channels. Flow boiling experiments were conducted for degrees of subcooling of 10 and 20 °C and mass fluxes equal to 400, 600, and 1000 kg/m^{2}s. Values of CHF and HTC during the experiments reached up to 72.8 W/cm^2 and 16.8 kW/m^{2}K, with total pressure drop lower than 10 kPa. The obtained results show that increase in mass flux caused increase in CHF, but at the cost of higher wall superheats and consequently lower HTC at low heat fluxes. However, as the higher mass flux enables the dissipation of higher heat fluxes and HTC increases with heat flux, the maximum HTC was achieved at the highest mass flux. Inlet subcooling had similar effects as mass flux, which was attributed to the portion of the heat sink in which phase-change effectively occurred.*

Keywords: *Cooling, Heat Sink, HFO, low-GWP, Microfluidics.*

1. INTRODUCTION

The development of novel cooling solutions for electronic components has been frequently investigated over the last decades. Expressive advances in electronics occurred with refined fabrication techniques that enabled the miniaturization of devices with increase in the density of transistors. Naturally, part of the electrical energy consumed by these devices is converted into heat and the working temperature of electronic equipments must be kept within constrict limits that ensure they will not fail. Thus, there is an increasing demand for efficient heat sinks, able to dissipate high heat loads from restricted spaces with low temperature variation. Among many strategies that have been proposed for electronics cooling, flow boiling in microchannels has promising characteristics to fulfill those demands, therefore much work has been done in order to improve the boiling heat transfer performance in multi-microchannels heat sinks, and dissipation of heat fluxes higher than 1 kW/cm^2 is already attainable.

As demonstrated by Tuckerman and Pease (1981) in their pioneering work, the flow of liquids inside multiple microchannels results in thermal resistances that are much lower than that from conventional air-cooling technologies, thus a proportional much higher global heat transfer coefficient (HTC), which is mainly related to higher thermal properties of liquids than those from air and to significant increase in effective heat transfer area promoted by microstructures. If the liquid that flows inside microchannels-based heat sinks is heated up to boiling conditions, the HTC increases even further because of latent heat exchange, and since the temperature of the fluid during phase-change at a given pressure is constant, this process induces lower thermal gradients than single-phase flows. Based on these aspects and in the required pumping power, Ribatski et al. (2007) concluded that flow boiling in heat sinks with microchannels constitute a more effective cooling solution than liquid flows. In addition, the operation range can be set such that

increases in heat flux are promptly accompanied by the activation of nucleation sites, so small or no variation of wall superheat can be noticed due to this self-regulating mechanism that induce less stresses due to thermal fatigue. However, some issues were observed in early investigations that hindered possible applications, like prohibitively high values of pressure drop (Δp) and early critical heat flux (CHF), strongly linked to excessive flow and thermal instabilities (Kandlikar, 2002).

The availability of imaging technology with consistently higher spatial and temporal resolutions and advances in fabrication techniques were essential in revealing some of the phenomena responsible for the occurrence of dryout and enabling the fabrication of geometries that could minimize deleterious effects and improve the overall heat transfer performance of flow boiling in microchannel heat sinks. Despite the apparently inevitable analogy between Δp and HTC, some enhancement strategies were successful in improving all desired aspects of flow boiling in multi-microchannels, resulting in augmented HTC and CHF and reduced Δp with less or not observable instabilities. Generally, these strategies are associated with the organization of the normally chaotic two-phase flow, like the implementation of artificial nucleation sites that define specific spots where bubbles will nucleate and grow, and phase-separation techniques, like vapor venting (Moreira et al., 2020).

Passive vapor venting techniques like open microchannels and diverging sections are relatively simple to apply and can be combined with any enhanced surface. Kandlikar et al. (2013) proposed a configuration consisting of open straight microchannels with diverging manifold and achieved a heat dissipation of 506 W/cm^2 with maximum HTC of 290 kW/m^{2}K in experiments with stable flow of water. Later, Kalani and Kandlikar (2014, 2015a, 2015b, 2016) observed that such configuration resulted in very high values of CHF that surpassed 1 kW/cm^2 with pressure drop lower than 50 kPa, which was attributed to a pressure recovery mechanism due to bubble growth in the expanding region. Lu and Pan (2008, 2009, 2011) and Tamanna and Lee (2015a, 2015b) also observed enhancements of diverging cross-sections in flow boiling experiments with water, with stable flows, lower pressure drop, higher HTC and CHF if compared to corresponding uniform cross-sections. Despite the impressive heat dissipation achieved with water, it should be mentioned that its saturation temperature at atmospheric pressure is too high for general working conditions in electronics, thus fluids with lower saturation temperatures can be more suitable to this application, but generally have poorer thermal properties than water and the performances achieved with these fluids are usually much lower than those reported for experiments with water. Besides, it should be mentioned that water is relatively cheap and readily available with many thermal properties that are desirable for heat transfer applications, thus it is used in most investigations in the literature.

In this context, the purpose of this work is to study the flow boiling behavior of the refrigerant R1336mzz(Z) in a microchannels-based heat sink with an open and divergent manifold through the evaluation of HTC, CHF and pressure drop. Experiments were carried out at a working pressure of 135 kPa, inlet subcooling equal to 10 and 20 °C, and for mass fluxes of 400, 600 and 1000 kg/m^{2}s. The experimental data was acquired at steady state and for each condition the applied heat flux was gradually increased up to CHF conditions.

2. MATERIALS AND METHODS

The commercial fluid Opteon™ 1100 from Chemours™ was selected as the working fluid for the experiments. This fluid is a new generation hydrofluoroolefin (HFO), R1336mzz(Z), with 0 ODP and low GWP, with properties that allow it to promptly replace commonly used hydrofluorocarbon (HFC) and hydrochlorofluorocarbon (HCFC) solutions in thermal management and waste heat recovery applications. Table 1 presents some properties of interest of this working fluid.

Table 1. Thermal properties of R1336mzz(Z).

Property	Value
Boiling point at 135 kPa [°C]	41,5
Liquid density at 20°C [kg/m^3]	1378
Vapor density at 20°C [kg/m^3]	4,21
Liquid viscosity at 20°C [mPa.s]	0,312
Vapor viscosity at 20°C [mPa.s]	0,011
Vapor Pressure at 20°C [kPa]	60
Liquid thermal conductivity at 20°C [W/m K]	0,0908
Vapor thermal conductivity at 20°C [W/m K]	0,0104
Liquid specific heat at 20°C [kJ/kg K]	1,23
Vapor specific heat at 20°C [kJ/kg K]	0,82
Critical temperature [°C]	171,3

Critical pressure [kPa]	2900
Heat of vaporization [kJ/kg]	163
Surface tension[N/m]	0,13
Global warming potential (GWP)	2
Ozone depleting potential (ODP)	0

Flow boiling experiments in copper heat sinks containing multi-microchannels were conducted at 137 kPa. The temperature of the surroundings was kept at 20 °C. A summary of the experimental conditions is presented in Table 2. All data was acquired at steady state, which was verified after the measured temperatures were constant for 10 minutes.

Table 2. Experimental conditions.

Condition	**Value**
Degree of subcooling [°C]	10 and 20
Mass flux [kg/m^{2}s]	400, 600 and 1000
Effective heat flux [W/cm^2]	up to 72,8
Wall temperature [°C]	up to 81,7

2.1 Experimental procedure

The main flow loop of the experimental apparatus for single-phase and flow boiling tests is presented in Figure 2. A micropump drives the fluid through a Coriolis flow meter that is used to measure the flow rate, then it flows through the pre-heater that establishes the desired state at the inlet of the test section and a sight glass where the single-phase liquid flow is verified. After the sight glass, the fluid goes into the test section and absorbs the heat supplied by the DC source, then reaches the plate heat exchanger that defines the working pressure, and finally gets to a counter-current double pipe heat exchanger, which is connected to a thermostatic bath containing water and set at 5 °C to ensure that subcooled liquid enters the pump, as can be verified on the sight glass downstream. A secondary loop with controlled temperature flows through the plate heat exchanger, such that the working pressure is set based on the desired saturation temperature.

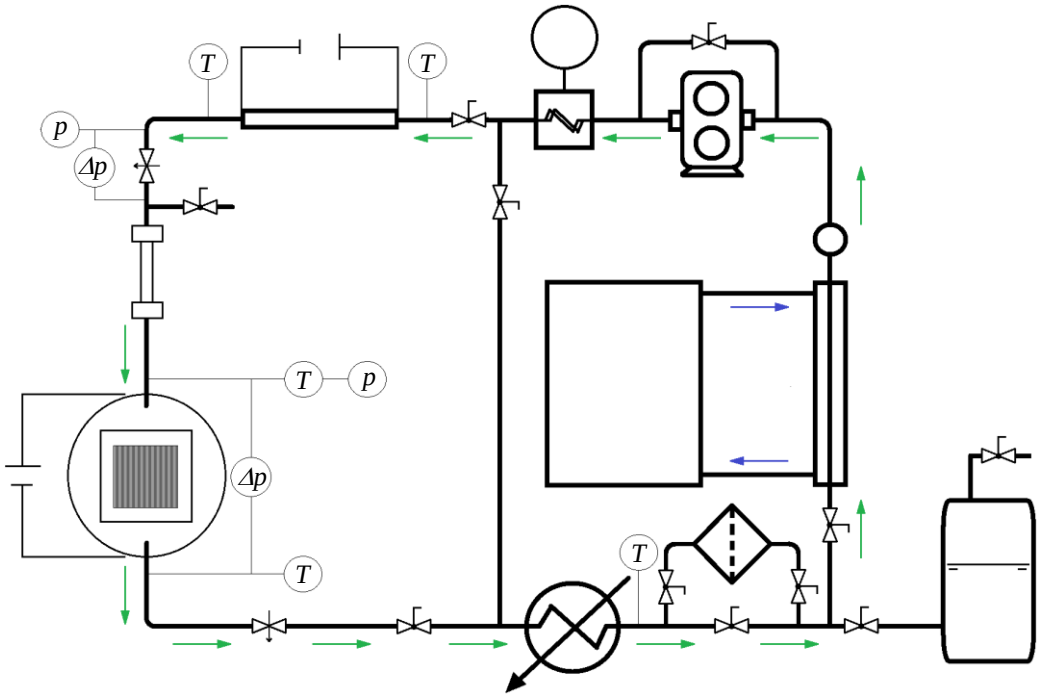

Figure 1. Schematic diagram of the main flow loop of the experimental apparatus.

Besides temperature and pressure measurements in the test section, additional instrumentation was used along the loop so the whole cycle could be monitored. Thus, an absolute pressure transducer was used to determine the states of the fluid before and after the pre-heater, together with thermocouples immersed in these positions. In addition, another immersed thermocouple measured the fluid temperature downstream the plate heat exchanger and a differential pressure transducer measured the pressure drop along the needle valve upstream the test section, employed to promote flow stability.

To run an experiment, first the fluid from the tank was loaded in the flow loop and the auxiliary circuit was set to flow through the plate heat exchanger at the desired saturation temperature, so the working fluid was heated and the working pressure increased. Then the preheater and the water flow from the thermostatic bath were turned on, so the inlet conditions were achieved, and finally the DC source was set. Once the readings from thermocouples embedded in the copper heater and in the test section were stable, which was verified by a variation within the expected precision error, steady state was considered and data points were acquired after 10 minutes. After that, the power in the DC source was risen and new data points were acquired at steady state until CHF was reached. Single-phase experiments were carried out in order to validate the experimental procedure and reveal the expected heat loss during flow boiling.

2.2 Test section

The test section was composed by a copper chip containing the microchannels and a polysulfone cover that was responsible for limiting the flow region and forming the open and diverging manifold. The copper chip was heated through the contact with a copper block containing eight embedded cartridge heaters (80W at 24V) connected to a DC current power source and these components were assembled in Celeron™ and Teflon™ insulating layers and an external aluminum support secured by screws. After the whole assembly was connected to the main flow loop of the experimental apparatus, another insulation layer composed by glass wool and elastomeric foam was added to reduce heat losses and the influence of potential variation of environmental temperature. Figure 1 depicts the copper chip and shows pictures of the test section in the experimental setup. The microchannels were CNC milled on top of the 10 mm x 10 mm square footprint, and three holes were drilled to lodge thermocouples. An alumina-based thermal grease was applied at the interface between the heater and the chip, and the thermal resistance between the cartridge heaters and the copper block was reduced using graphite.

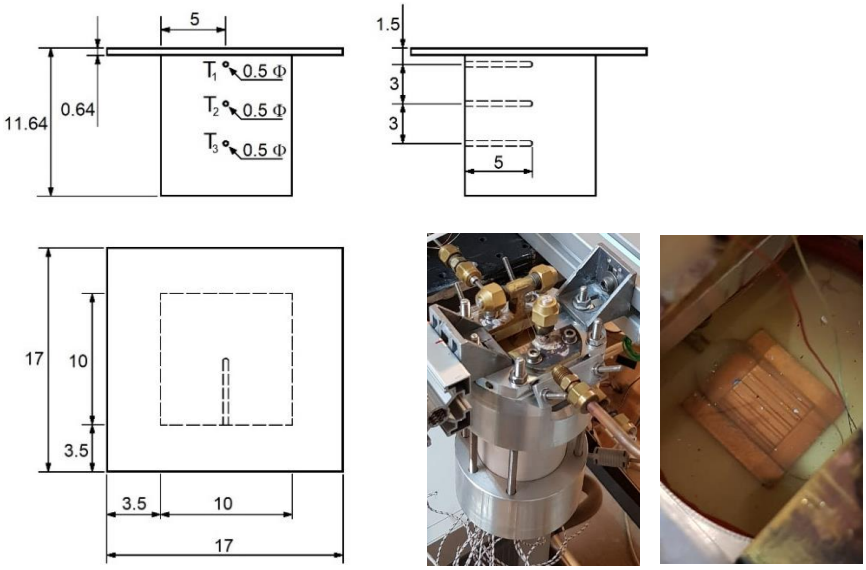

Figure 2. Design of the copper chip with microchannels and photographs of the assembled test section. The 10 mm x 10 mm dashed square corresponds to the footprint.

The three thermocouples embedded in the copper chip were used to estimate the wall temperature during the experiments and to provide guess values of heat flux in the iterative procedure to estimate the heat loss and the heat transfer coefficient. Immersed thermocouples recorded the fluid temperatures at inlet and outlet sections, and an additional thermocouple was housed in the copper heater to guarantee that the temperature of the block was below 200 °C and the cartridge heaters worked within a safe temperature range. All thermocouples used in the experiments were calibrated K-type thermocouples with uncertainties of 0.13 °C. An absolute pressure transducer was used to record the pressure at the inlet region of the test section and a differential pressure transducer measured the pressure drop along the channels´ region with uncertainties of 0.13 and 0.01 kPa, respectively.

2.3 Data reduction

For single-phase tests, the heat flow absorbed by the fluid was calculated based on the mass flow rate and specific enthalpies at inlet and outlet positions:

$$\dot{Q}_{abs} = \dot{m}[i_{out} - i_{in}] \tag{1}$$

The absorbed heat flow was subtracted from the power applied by the DC source ($\dot{Q}_{DC}$) in order to reveal the heat loss ($\dot{Q}_{lost}$) for various conditions:

$$\dot{Q}_{lost} = \dot{Q}_{DC} - \dot{Q}_{abs} \tag{2}$$

and the relative loss was also calculated:

$$\dot{Q}_{lost\_rel} = \frac{\dot{Q}_{lost}}{\dot{Q}_{DC}} \tag{3}$$

The effective heat transfer coefficient (h) was calculated using Newton´s Law of Cooling

$$h = \frac{\dot{Q}_{abs}}{A(T_w - T_f)} \tag{4}$$

where A is the wetted area and T_w and T_f are respectively the wall and fluid temperatures, assessed through the thermocouples measurements and given by:

$$T_w = \frac{T_1+T_2+T_3}{3} + \frac{\dot{Q}_{abs}}{A}\frac{1.5+4.5+7.5}{3k_{Cu}} \tag{5}$$

$$T_f = \frac{T_{in}+T_{out}}{2} \tag{6}$$

The relative heat losses in single-phase experiments were related to the heat transfer coefficient and, as expected, they are higher for low values of h and present an asymptotic behavior for high values of h, as displayed in Fig. 3. Thus, an empirical correlation for $\dot{Q}_{lost\_rel}$ as a function of h was obtained, and the expression seen in Equation (7) was used to calculate heat losses for subsequent flow boiling experiments:

$$\dot{Q}_{lost\_rel} = 0.27304 + \frac{1}{e^{h/608}} \tag{7}$$

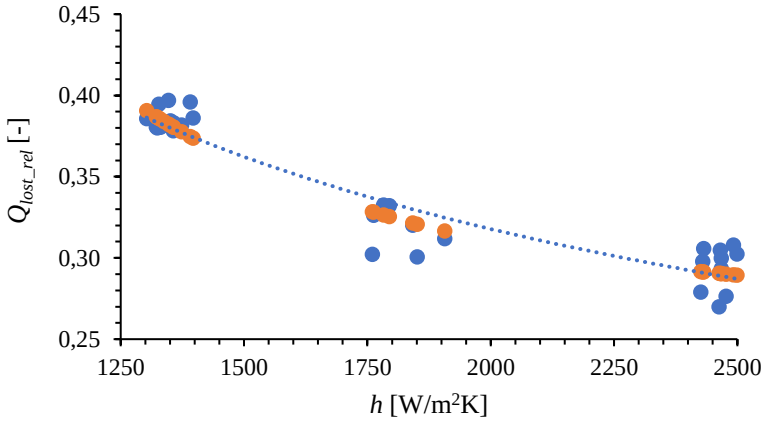

Figure 3. Relative heat losses versus heat transfer coefficients obtained experimentally in single-phase experiments together with the empirical curve fitted to the whole dataset.

Since the empirical correlation from Eq. (7) depends on the value of h, iterative calculations were necessary to determine both the relative heat losses and the values of heat transfer coefficient in flow boiling experiments. During the iterative process, the heat flow absorbed by the fluid and the wall temperature were calculated combining Equations (2) and (3) and using Equation (5), and the heat transfer coefficient was updated with Equation (4).

3. RESULTS AND DISCUSSION

Figure 4 presents the boiling curve obtained for the six experimental conditions that were investigated. The footprint heat flux (q_{fp}") is calculated based on the heat provided by the DC source subtracted by the calculated heat losses, considering the footprint area, and the wall superheat (ΔT_w) was calculated as the temperature difference between the wall and the fluid, respectively given by Equations (5) and (6). As can be observed, increases in mass flux and in the degree of subcooling resulted in higher values of CHF, with a maximum of 72.8 W/cm^2 dissipated at 1000 kg/m^{2}s with 20 °C of inlet subcooling. However, it is also possible to observe that the wall superheats achieved at superior mass fluxes and degree of subcooling are greater than the values observed for low mass flux and degree of subcooling, which yields lower values of HTC.

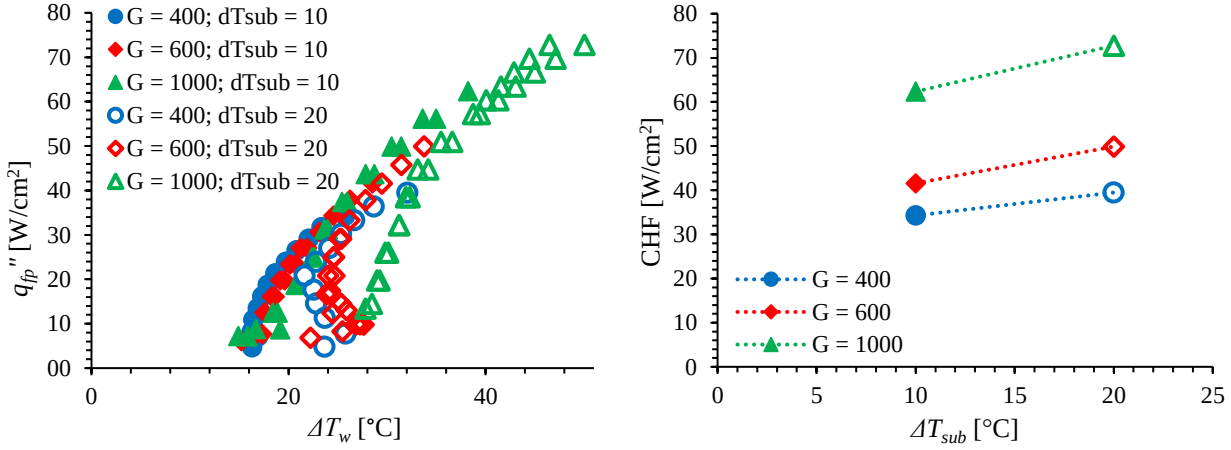

Figure 4. Boiling curve of R1336mzz(Z) (left) and critical heat flux (right) achieved in all experimental conditions.

In addition, the effect of mass flux is more pronounced for the subcooling of 20 °C and it is possible to observe a reduction in wall superheat with increase of heat flux for lower mass fluxes at this subcooling. This is attributed to the activation of more nucleation sites as the power is increased and also the wall superheat at first, but then, with more active cavities, the higher nucleation activity reduced the wall superheat, and with previous vapor nuclei in these cavities the required energy to keep them active is lower, thus they remain active even at lower wall superheats. The effects of mass flux and inlet subcooling can be further analyzed through HTC calculations and pressure drop measurements, as displayed in Figure 5.

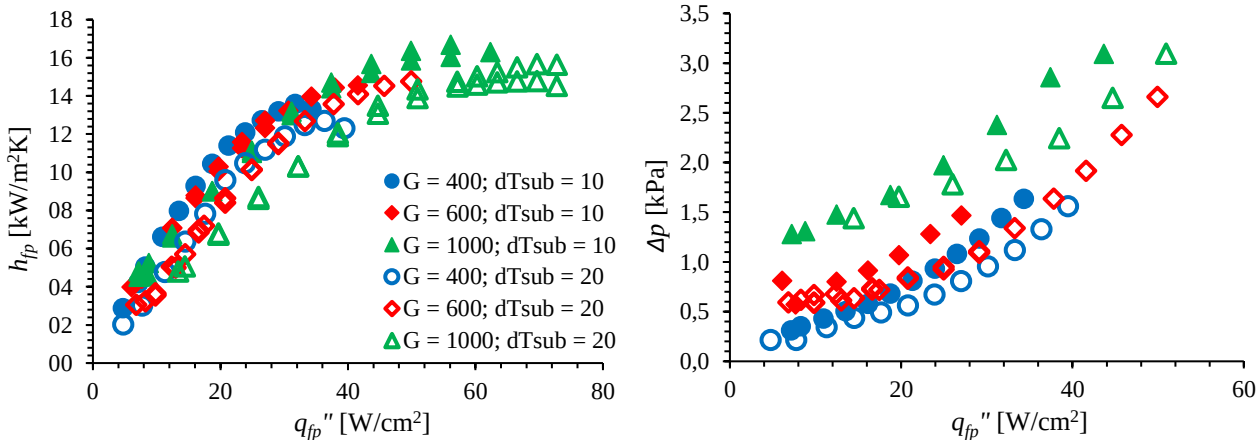

Figure 5. Heat transfer coefficient (left) and pressure drop (right) as functions of footprint heat flux for all experimental conditions.

As was inferred by the data from Figure 4, it is possible to observe in Figure 5 that the HTC is higher for the lower superheat and that it increases with decrease in mass flux, which can be attributed to the phase-change flow occurring in a larger portion of the microchannels that results in augmented heat transfer. Nevertheless, since the higher mass flux enables the dissipation of higher heat fluxes, the maximum value of HTC was achieved at the highest mass flux. It should be mentioned that the HTC increases almost asymptotically with heat flux up to a maximum that was reached right before

CHF was achieved, suggesting that convective boiling mechanisms are dominant in these experiments. Pressure drop data presented in Figure 5 corroborates the idea that differences observed in HTC are due to how much of the heat sink is effectively occupied by phase-change flow. Naturally, the pressure drop increases with mass and heat fluxes, because of inertia forces and effective density variation, respectively. Moreover, higher inlet subcooling results in lower pressure drop, since there will be less vapor occupying the volume of the heat sink.

4. CONCLUSIONS

This work presented some heat transfer and pressure drop results of flow boiling of R1336mzz(Z) in a heat sink consisting of copper microchannels and an open and divergent manifold. Experiments were conducted for increasing heat flux at three mass fluxes and two values of inlet subcooling. According to the present data, increases in mass flux and inlet subcooling resulted in higher CHF, but lower HTC. The observed behavior was related to the portion of the heat sink in which phase-change flow effectively occurred. The highest value of HTC was 16.7 kW/m^2K and the highest CHF was 72.8 W/cm^2, both at 1000 kg/m^2s, but the first was achieved at the inlet subcooling of 10 °C while the latter at 20 °C. Pressure drop was lower than 10 kPa during all experiments.

5. ACKNOWLEDGEMENTS

The authors would like to acknowledge the financial support provided by CNPq and FAPESP (Grants 2015/24834-3, 2016/09509-1, 2017/12576-5, 2018/23538-0). The technical support given by Craig Arnold and Rick Würzer, from RIT´s ME Department, and by José Roberto Bogni and Jorge Nicolau dos Santos, from EESC-USP's Department of Mechanical Engineering is also recognized and deeply appreciated.

6. REFERENCES

Kalani, A., Kandlikar, S. G., 2014. "Evaluation of pressure drop performance during enhanced flow boiling in open microchannels with tapered manifolds". *Journal of Heat Transfer*, Vol. 136, p. 051502.

Kalani, A., & Kandlikar, S. G., 2015a. "Combining liquid inertia with pressure recovery from bubble expansion for enhanced flow boiling". *Applied Physics Letters*, Vol. 107, p. 181601.

Kalani, A., & Kandlikar, S. G., 2015b. "Effect of taper on pressure recovery during flow boiling in open microchannels with manifold using homogeneous flow model". *International Journal of Heat and Mass Transfer*, Vol. 83, p. 109-117.

Kalani, A., & Kandlikar, S. G., 2016. "Heat dissipation beyond 1 kW/cm^2 with low pressure drop and high heat transfer coefficient for flow boiling using open microchannels with tapered manifold". In *Proceedings of the ASME 2016 14th International Conference on Nanochannels, Microchannels, and Minichannels, ICNMM 2016*, Washington, DC, USA.

Kandlikar S. G., 2002. "Fundamental issues related to flow boiling in minichannels and microchannels". *Experimental Thermal and Fluid Science*, Vol. 26, p. 389-407.

Kandlikar, S. G., Widger, T., Kalani, A., Mejia, V., 2013. "Enhanced flow boiling over open microchannels with uniform and tapered gap manifolds". *Journal of Heat Transfer*, Vol. 135, p. 061401.

Lu, C. T., & Pan, C., 2008. "Stabilization of flow boiling in microchannel heat sinks with a diverging cross-section design". *Journal of Micromechanics and Microengineering*, Vol. 18, p. 075035.

Lu, C. T., & Pan, C., 2009. "A highly stable microchannel heat sink for convective boiling". *Journal of Micromechanics and Microengineering*, Vol. 19, p. 055013.

Lu, C. T., & Pan, C., 2011. "Convective boiling in a parallel microchannel heat sink with a diverging cross section and artificial nucleation sites". *International Journal of Heat and Mass Transfer*, Vol. 35, p. 810-815.

Moreira, D.C., Ribatski, G., Kandlikar, S.G., 2020. "Review of enhancement techniques with vapor extraction during flow boiling in microchannels". In *Proceedings of ASME 2020 18th International Conference on Nanochannels, Microchannels and Minichannels ICNMM2020*, Orlando, Florida, USA.

Ribatski, G., Cabezas-Gómez, L., Navarro, H. A., Saíz-Jabardo, J. M., 2007. "The advantages of evaporation in micro-scale channels to cool microelectronic devices". *Thermal Engineering*, Vol. 6, p. 34-39.

Tamanna, A., & Lee, P. S., 2015a. "Flow boiling heat transfer and pressure drop characteristics in expanding silicon microgap heat sink". *International Journal of Heat and Mass Transfer*, Vol. 82, p. 1-15.

Tamanna, A., & Lee, P. S., 2015b. "Flow boiling instability characteristics in expanding silicon microgap heat sink". *International Journal of Heat and Mass Transfer*, Vol. 89, p. 390-405.

Tuckerman, D. B., & Pease, R. F. W., 1981. "High-performance heat sinking for VLSI". *IEEE Electron device letters*, Vol. *2*(5), p. 126-129.

7. RESPONSIBILITY NOTICE

The authors are the only responsible for the printed material included in this paper.